

IMECE2006-14641

**DILUTION AND SUPPRESSION OF PARTIALLY PREMIXED FLAMES IN NORMAL
AND MICROGRAVITY FOR DIFFERENT FUELS**

ANDREW J. LOCK

Mechanical and Industrial Engineering,
University of Illinois at Chicago,
Chicago, IL, USA
alock1@uic.edu

ALEJANDRO BRIONES

Mechanical and Industrial Engineering,
University of Illinois at Chicago,
Chicago, IL, USA
abrion1@uic.edu

SURESH K. AGGARWAL

Mechanical and Industrial
Engineering,
University of Illinois at Chicago,
Chicago, IL, USA
ska@uic.edu

ISHWAR K. PURI

Engineering Science and
Mechanics,
Virginia Polytechnic Institute and
State University,
Blacksburg, VA, USA
ikpuri@vt.edu

UDAY G. HEGDE

National Center for Space
Exploration Research,
NASA Glenn Research Center,
Cleveland, OH, USA
uday.g.hegde@grc.nasa.gov

ABSTRACT

The suppression of fires and flames is an important area of interest for both terrestrial and space based applications. In this investigation we elucidate the relative efficacy of fuel and air stream inert diluents for suppressing laminar partially premixed flames. A comparison of the effects of fuel and air stream dilution are also made with other fuels. Both counterflow and coflow flames are investigated, with both normal and zero-gravity conditions considered for coflow flames. Simulations are conducted for both the counterflow and coflow flames, while experimental observations are made on the coflowing flames. With fuel or air stream dilution, coflow flames are observed to move downstream from the burner after overcoming initial heat transfer coupling. Further increases in diluent result in increases in the flame liftoff height until blow off occurs. The flame liftoff height and the critical volume fraction of extinguishing agent at blow out vary with both equivalence ratio and with the stream in which diluents are introduced. Nonpremixed methane-air flames are more difficult to extinguish than partially premixed flames with fuel stream dilution; whereas, partially premixed methane-air flames are more resistant to extinction than nonpremixed flames with air stream dilution. This difference in efficacy of the fuel and air stream dilution is attributed to the action of the diluent. In leaner partially premixed flames with fuel stream dilution and richer partially premixed flames with air stream dilution the effect of the diluent is to replace the deficient reactant in the

system, thus starving the flame. In leaner partially premixed flames with air stream dilution and richer partially premixed flames with fuel stream dilution the effect of the diluent is purely thermal in that it absorbs heat from the flame, until combustion may no longer be sustained. The dilution effect is more effective than the thermal effect. When gravity is eliminated from the 2-D flame the liftoff height decreases and the critical volume fraction of diluent for blow off is also decreased.

INTRODUCTION

Flame extinction is important from both fundamental and practical considerations. Therefore, several analytical, numerical, and experimental investigations have focused on the strain-induced extinction of counterflow partially premixed flames (PPFs) and nonpremixed flames (NPFs) [1,2]. The counterflow geometry is useful in this respect, since it affords control over both the strain rate and flame position [3]. Consequently, the agent concentration requirements for the suppression of counterflow flames at low strain rates are of interest, because they may correspond to the limiting extinction requirements for axisymmetric cup burner flames [4] that more closely model real fire scenarios. Most previous investigations have characterized the air stream agent requirements for the suppression of NPFs. There has been very little investigation

on the fuel stream agent requirements for the suppression of PPFs, especially in a cup burner or coflow configuration.

Bundy et al. [5] investigated the fuel and air stream agent (N_2 , CO_2 , and CF_3Br) requirements for the suppression of low strain rate counterflow NPFs. They found that the air stream diluted NPFs extinguish at a lower diluent mole fraction compared to the corresponding fuel stream diluted NPFs. Trees et al. [6] Investigated the chemical inhibition of NPFs by CF_3Br (Halon-1301) and suggested that the difference between the fuel and air stream effectiveness of a diluent could be attributed to preferential diffusion effects. Since their diluent was not chemically inert, it is yet unclear if the difference between the fuel and air stream effectiveness by inert agents (such as N_2 , and CO_2) is due to diffusive effects.

Flame extinction can generally be achieved through three methods [7]: (1) reducing the oxygen or fuel concentration so that combustion ceases (dilution effect); (2) reducing the temperature so that no free radicals are formed (cooling effect); and (3) reducing the free radical concentration and thus interrupting the flame chemistry (chemical effect). In this context, chemically inert suppressant agents can also extinguish fires by physical means, i.e., like CO_2 , they can also have dilution and cooling effects.

Halons have been very successful as chemically active flame suppression agents but have significant ozone layer depletion potential [8]. Therefore, CO_2 , which is essentially chemically inert, is considered in this investigation. It is also used as a fire-suppressant agent in the US modules of the International Space Station which justifies the investigation of microgravity conditions.

There is a likelihood that fires can originate in the partially premixed mode when a pyrolyzed or evaporated fuel forms an initial fuel rich mixture with the ambient air. Hence, partially premixed combustion must be considered in the context of fire safety [9]. Previous studies have shown that the structure of PPFs can be modified significantly by changing the level of partial premixing [10]. Seiser et al. [11] found that premixing of one or both reactant streams of a NPF with the other reactant has a significant influence on PPF extinction. They also observed that in comparison with NPFs, PPFs are more difficult to extinguish if fuel is added to the oxidizer stream, while PPFs are easier to extinguish if oxygen is added to the fuel stream of a NPF.

Previous work by Masri and Seshadri has investigated the effects of fuel and air stream dilution on nonpremixed flames of different fuels including methane, ethylene and acetylene [12,13]. They found that the relative effectiveness of fuel and air stream dilution varies with the type of fuel being considered. Specifically they review literature which suggests that the ratio of Hydrogen to Carbon atoms in the fuel affects the relative effectiveness of fuel and air stream dilutions. It is asserted that for nonpremixed methane-air flames that air stream dilution is more effective than fuel stream dilution, while fuel and air stream dilution are equally effective for

ethylene-air flames when the chemically active suppressant Halon 1301 is used.

The effects of gravity on coflow flame liftoff and blowout are important for fire safety. As mentioned previously, most fire safety research has focused on the introduction of reacting and nonreacting diluents into the coflowing air stream surrounding a nonpremixed flame. Takahashi et. al. [20] and others have investigated the effects of gravity on the liftoff and extinction of nonpremixed flames with air stream dilution, and Lock et al. [14] have investigated the effect of diluting the fuel stream of a PPF on flame liftoff and blowout. This previous work has found that flames, with fuel stream or air stream dilution, require more diluent for liftoff and blowout in microgravity. A portion of our focus is the comparison of fuel stream and air stream dilution under both microgravity and normal gravity conditions.

The preceding discussion indicates that partial premixing of fuel and oxidizer is of common occurrence in many fires. However, there is relatively little fundamental information available on the extinction characteristics of PPFs, since most previous investigations have focused on the extinction of NPFs. Moreover, previous studies have not examined the effectiveness of fuel stream dilution versus air stream dilution in flame extinguishment, especially in the context of PPFs. The major objective of our investigation is to characterize the effectiveness of air stream and fuel stream dilutions in extinguishing nonpremixed and partially premixed flames. In order to examine the configuration-dependent similarities or differences, both coflow and counterflow flames are considered.

EXPERIMENTAL METHOD

Laminar methane-air flames were established in our laboratory on a coannular burner with an inner diameter of 11.1 mm and an outer annulus diameter of 22.2 mm, depicted in Fig. 1. The burner has several fine wire mesh inserts placed in the two ducts to produce a plug flow velocity profile. Both the fuel and air stream velocities were maintained at 0.5 m/s. The fuel-air mixtures as well as the diluents were premixed before each experiment in order to assure consistent composition. The fuel-air-diluent mixtures are accurate to within 1% of the volumetric flow rate. The fuel rich mixture was introduced through the inner duct and air through the outer annulus of the burner. The CO_2 diluent was introduced into the fuel stream or the air stream of the flame in order to compare the effectiveness of fuel and air stream dilution. Temporal measurements were made using a digital camera (30 fps; 640×480 pixels). The flames generally exhibited well-organized oscillations due to buoyant acceleration in normal gravity. The flame liftoff height was determined by locating the displacement of the maximum chemiluminescence (representing the flame reaction kernel) from the burner rim. Experimental error in the measurement of liftoff height is limited by the resolution of the images.

Generally, the measurement error is no more than $\pm 1\%$ of the value reported for liftoff height, L_f .

C_2^* chemiluminescence images are taken with an Andor iStar Intensified CCD (ICCD) camera with a $473\pm 10\text{nm}$ bandpass filter. The C_2^* chemiluminescence images are post processed by a Matlab program which normalizes the image and applies the Able inversion. The Able inversion is a tomographic inversion for reproducing the internal structure of an axisymmetric object from its integrated emissive projection, e.g. as observed by the ICCD camera [15]. C_2^* chemiluminescence has been shown to indicate the reaction zones within the flame [16, 17].

Microgravity experiments were conducted in the 2.2 second drop tower at the NASA Glenn Research Center in Cleveland, OH. The microgravity rig, shown in Fig. 1, was used for both normal- and microgravity experiments and has been described elsewhere [14]. In the drop tower the fuel, air, and diluents are premixed in the onboard cylinders of the rig. An onboard microprocessor controls the sequence of events including starting the gas flow, igniting the flow, and collecting any onboard telemetry. Video is obtained using an onboard color CCD camera and recorded on a MiniDV recorder.

COMPUTATIONAL METHOD

Axisymmetric coflow flames were simulated using a computational model developed by Katta et al. [16,17]. The model solves the time-dependent governing equations for unsteady reacting flows in an axisymmetric configuration that can be written in a generalized form as:

$$\frac{\partial(\rho\Phi)}{\partial t} + \frac{\partial(\rho u\Phi)}{\partial r} + \frac{\partial(\rho v\Phi)}{\partial z} = \frac{\partial}{\partial r} \left(\Gamma^\Phi \frac{\partial\Phi}{\partial r} \right) - \frac{\partial}{\partial z} \left(\Gamma^\Phi \frac{\partial\Phi}{\partial z} \right) - \frac{\rho\Phi}{r} + \frac{\Gamma^\Phi}{r} + \frac{\partial\Phi}{\partial r} + S^\Phi$$

Here t denotes the time, and u and v the axial (z) and radial (r) velocity components, respectively. The general form of the equation represents conservation of mass, momentum, species, or energy conservation, depending on the variable used for Φ . The diffusive transport coefficient Γ^Φ and source terms S^Φ are described in Ref. 16. Introducing the overall species conservation equation and the state equation completes the equation set. A sink term based on an optically thin gas assumption was included in the energy equation to account for thermal radiation from the flame in the form $q_{rad} = -4\sigma K_p (T^4 - T_o^4)$ [18] where T denotes the local flame temperature, and K_p accounts for the absorption and emission from the participating gaseous species (CO_2 , H_2O , CO and CH_4) expressed as $K_p = P \sum_k X_i K_{p,i}$ where $K_{p,i}$ denotes the mean absorption coefficient of the k^{th} species. Its value was obtained using a polynomial approximation to the experimental data provided in Ref. 18.

The methane-air chemistry was modeled using a mechanism that considers 24 species and 81 elementary reactions [19]. The computational domain consisted of $150\text{mm} \times 100\text{mm}$ in the axial (z) and radial (r) directions, respectively, and contained a staggered, non-uniform grid system. The boundary conditions are described elsewhere [16, 17]. Once undiluted flames were established, CO_2 was gradually added in the fuel stream or the air stream until blowout occurs [20].

Simulations of counterflow methane-air and ethylene-air flames, established at various fuel stream equivalence ratios, global strain rates, and fuel and air stream dilutions, were performed using the CHEMKIN package [21]. The flame chemistry was modeled using the GRI-Mech 3.0 mechanism [22] for methane-air combustion and the San Diego mechanism [23] for ethylene-air combustion. The distance between the two nozzles was 2.54 cm. The fuel and oxidizer temperatures were assumed to be 300 K.

RESULTS AND DISCUSSION

The axisymmetric flame model has been previously validated against measurements for a variety of steady and unsteady flames, including opposed-jet diffusion flames [24], burner-stabilized [17,25], lifted jet flames [20], and microgravity flames [10,14,20]. We provide additional validation by comparing the predicted heat release rate contours with C_2^* chemiluminescence images for an undiluted and fuel stream $X_{\text{CO}_2}=0.10$ diluted methane-air PPFs established at $\phi=2.25$ and 1-g. As shown in Fig. 2, the numerical model reproduces the measured flame topology including the locations of the various reaction zones and the liftoff height for both the undiluted and the fuel stream diluted PPFs. The undiluted flame is burner attached and exhibits a double-flame structure (containing two reaction zones), namely the rich premixed (RP) and the nonpremixed reaction (NP) zones. Introducing diluent into the flame causes the flame to lift off from the burner. The flame structure then changes from that of a double to a triple flame structure, as reactants mixing is enhanced in the wake region above the burner rim, allowing entrainment of air into the fuel and vice versa which produces a third lean premixed reaction zone (LP). Both the 1-g simulations and measurements exhibit well-organized oscillations induced by buoyant acceleration and so care is taken in comparing any two flames at the same phase angle. No buoyant oscillations were observed in $\mu\text{-g}$.

The methane-air flame state relationships in terms of the major reactant and product species (CH_4 , O_2 , H_2O , and CO_2), and "intermediate" fuel species (H_2 and CO) profiles with respect to the mixture fraction (f) [26] for both coflow and counterflow flames are shown in Fig. 3. Scalar profiles for counterflow flame simulations at $\phi=1.5$, and ∞ , and a global strain rate of 100s^{-1} are compared with those for the corresponding coflow flames. Despite the different configurations, there is good similarity in the scalar profiles of

coflow and counterflow flames. Both the coflow and counterflow PPFs established at $\phi=1.5$ exhibit a double-flame structure while the nonpremixed coflow and counterflow flames exhibit a merged flame structure. As the level of partial premixing decreases (i.e., ϕ increases from 1.5 to ∞), the stoichiometric mixture fraction decreases from $f_s=0.68$ to 0.055. As the two reaction zones move closer to each other, the flame moves from the fuel side towards the air side, and the leakage of fuel (in form of intermediate species) is replaced by the leakage of oxygen through the flame [27]. Since mixture fraction is the ratio between the material originating from the fuel rich mixture to the total mass, the stoichiometric mixture fraction (f_s) indicates if the flame is located in a region of high or low concentration of material originating from the fuel rich mixture. For $f_s>0.5$, there is more material from the fuel rich mixture and again leakage of fuel is present, whereas for $f_s<0.5$, there is more material from the air side and leakage of oxygen through the flame occurs. As it will be shown f_s plays an important role on the fuel and air stream extinction characteristics.

Fuel Stream Dilution verses Air Stream Dilution

Fig. 4 presents the measured and predicted liftoff heights as a function of CO_2 mole fraction for coflow flames established at $\phi=1.5$, 2.25 (PPFs) and ∞ (NPF) in 1-g and μ -g. There is generally good agreement between predictions and measurements. Although the measured and predicted liftoff heights at blowout do not quantitatively agree, the critical CO_2 mole fraction required for blowout (extinction) is accurately predicted. Moreover, at lower liftoff heights, there is better agreement between the measured and predicted flame liftoff heights. The quantitative differences are probably due to the inflow boundary conditions, the geometric characteristics of the isothermal insert [17], and uncertainties in the liftoff height measurements. Nonetheless, there are some important observations from Fig. 4:

(1) The undiluted coflow NPF is lifted and stabilized downstream of the burner rim, while the PPFs are stabilized at the burner rim. The variation of liftoff height with the CO_2 mole fraction and critical CO_2 mole fraction at blowout depend strongly on the level of partial premixing. The predicted fuel stream CO_2 dilutions required for flame blowout at $\phi=1.5$, 2.25, and ∞ are $X_{\text{CO}_2}=0.12$, 0.16, and 0.41, respectively.

(2) With air stream dilution, both the measurements and predictions indicate that the NPF lifts off rapidly from the burner and blows out when a relatively small CO_2 mole fraction is added (cf. Fig. 4b). On the other hand, the PPFs liftoff is initially gradual but becomes more rapid with increasing air stream dilution. For the results presented in Fig. 4b, the predicted air stream CO_2 dilutions required for the blowout of the flames established at $\phi=1.5$, 2.25 and ∞ are 0.5, 0.18, and 0.12, respectively. This clearly shows that NPFs are more difficult to extinguish than PPFs when they are diluted

with an inert agent in the fuel stream whereas PPFs are more difficult to extinguish when they are air stream diluted.

(3) The effect of gravity on the coflow flames is the same with both fuel stream and air stream dilution. When gravity is eliminated, the flame liftoff height is reduced due to the elimination of buoyant acceleration in the flame. Elimination of buoyant acceleration reduces the effective gas stream velocity and decreases the flame stretch at the flame front [14]. The critical CO_2 dilution for flame blowout also increases with decreased gravitational acceleration. This behavior is explained by the flame blowout hypothesis. That is that when the flame speed is impeded enough the flame can not stabilize in the flow and blows off. With the elimination of gravity the effective gas stream velocity is reduced due to the elimination of buoyant acceleration so that the flame can remain in the flow to a larger critical value.

Flame liftoff and blowout are complex processes involving transport, partial premixing, flame propagation, scalar dissipation and extinction [28]. Strain-induced flame extinction has been exhaustively investigated [2] and is now well understood, and thus, using counterflow simulations to explain jet flame blowout is well justified by the literature [5] as well as by our demonstration of the similarities in the state relationships of the coflow and counterflow flames, cf. Fig. 3. Therefore, we now use the counterflow flame results to explain the relative effectiveness of fuel or air stream dilution. Fig. 5 presents the critical CO_2 mole fraction required for the extinction of fuel and air stream diluted methane-air counterflow flames, as a function of inverse equivalence ratio, ϕ^{-1} , for several global strain rates (a_s). The blowout conditions for coflow flames are also presented in the figure. For both counterflow and coflow flames, the critical fuel stream CO_2 mole fraction required for extinction increases as ϕ is increased (ϕ^{-1} decreases) or the level of partial premixing is decreased. Conversely, the critical air stream CO_2 mole fraction required for the extinction of counterflow and coflow flames decreases as ϕ is increased (ϕ^{-1} is decreased). Thus, in spite of the differences in configuration, the effects of partial premixing and fuel and air stream dilution on the extinction of counterflow and coflow flames are similar. As indicated in Fig. 5, the critical CO_2 mole fraction for counterflow flame extinction decreases as the global strain rate is increased. This is to be expected, since the flow residence time decreases at higher strain rates while the radical losses from the flame increase. The net effect is that the flame temperature decreases, and, therefore, extinction is achieved with a lower diluent concentration for both fuel and air stream diluted flames. Consequently μ -g flames, where the global strain rate of the flame is decreased, can be more difficult to extinguish than 1-g flames.

Fig. 5 shows that fuel and air stream dilutions are equally effective in flame extinction when the equivalence ratio is around $\phi\approx 2.0$ regardless of the strain rate. At this equivalence ratio, the mole fractions of CH_4 and O_2 are nearly equal (i.e.

$X_{\text{CH}_4} = X_{\text{O}_2} = 0.1736$) and the stoichiometric mixture fraction is $f_s = 0.5274$ so that the flame lies almost at the spatial center of the fuel and air streams. Increasing the rich mixture equivalence ratio moves the two reaction zones closer to one another and the flame exhibits a nearly merged flame structure. When $\phi = \infty$, the NPF has a single reaction zone. For NPFs with $f_s < 0.5$ oxidizer leaks through the reaction zone while for $f_s > 0.5$ there is fuel leakage [27]. Therefore, for flames established at $f_s > 0.5$, fuel stream dilution is more effective than air stream dilution because the deficient reactant is the fuel, while for flames at $f_s < 0.5$, air stream dilution is more effective since the deficient reactant is oxygen.

When a PPF is fuel stream diluted, the maximum flame temperature, T_{max} , decreases linearly and rapidly because the diluent removes the deficient reactant (dilution effect) cooling the flame effectively. On the contrary, for air stream dilution, the diluent no longer removes the deficient reactant, but only cools the flame (thermal effect). Since the deficient reactant for the NPF is oxygen, the opposite extinction behavior is observed in terms of fuel and air stream dilutions. Consequently, a much higher diluent concentration is required for extinguishing the air stream diluted PPFs and the fuel stream diluted NPFs as compared to the requirements for extinguishing fuel stream diluted PPFs and the air stream diluted NPFs.

Effect of Fuel Type

Methane and ethylene are expected to have different critical diluent mole fractions at extinction. Fig. 6 plots the extinction diluent mole fractions for fuel and air stream dilution of experimental coflow flames and numerically predicted ethylene counterflow flames with a global strain rate of $a_g = 100\text{s}^{-1}$ and $a_g = 200\text{s}^{-1}$. Ethylene produces higher flame temperatures and flame speeds than methane and has a broader flammability limit. Because of the broader flammability limits Fig. 6 shows that the critical diluent mole fraction for extinction of ethylene-air flames will always be larger than that of methane-air flames, cf. Fig. 5. The critical diluent mole fraction for extinction of fuel and air stream diluted methane and ethylene flames are directly compared in Fig. 7 and plotted versus ϕ^{-1} as well as versus the stoichiometric mixture fraction of the undiluted flame, f_{st} . Ethylene always has a larger stoichiometric mixture fraction than methane which causes ethylene-air flames to be stabilized closer to the fuel side of a flame. Thus, fuel stream dilution is more effective than air stream dilution over a larger range of equivalence ratio. Fig. 7a illustrates that fuel and air stream dilution of the ethylene-air flame become equally effective at a larger value of ϕ (smaller value of ϕ^{-1}) than is observed for the methane-air flame. Fig. 7b presents the the critical diluent mole fraction for extinction for both methane-air and ethylene-air flames plotted versus f_{st} . While a distinct difference is noted in the location of the intersection of fuel and air stream dilution lines when plotted versus ϕ^{-1} , the difference is decreased when the same plot is

presented versus f_{st} . Both methane-air and ethylene-air flames' fuel and air stream dilution become equally effective near $f_{st} = 0.5$ which indicates that the relative effectivity of fuel and air stream dilution can be explained regardless of the fuel type by looking at the undiluted flame's stoichiometric mixture fraction.

CONCLUSIONS

An experimental and computational investigation is performed on the effectiveness of fuel stream dilution versus air stream dilution in extinguishing laminar methane-air and ethylene-air flames using the chemically inert fire suppressant agent CO_2 . The extinction of both partially premixed (PPF) and NPFs (NPF) in coflow (for methane-air flames at 1-g and μ -g and ethylene-air flames at 1-g) and counterflow (for both methane- and ethylene-air flames) configurations has been considered. In order to explain the differences between the extinction characteristics of fuel stream and air stream diluted flames, the critical CO_2 mole fraction for the blowout (extinction) of jet flames was compared with that for the extinction of counterflow flames. The extinction of methane-air and ethylene air flames is also compared.

As the level of partial premixing is decreased (i.e., ϕ is increased) the stoichiometric mixture fraction decreases, the two reaction zones move closer to each other, and the leakage of fuel from the rich premixed zone to the nonpremixed reaction zone decreases, while the leakage of oxygen increases. The stoichiometric mixture fraction (f_s) clearly predicts the leakage of fuel and oxygen when f_s is approximately $f_s > 0.5$ and $f_s < 0.5$, respectively, and can be used to explain differences between the extinction of fuel stream and air stream diluted flames.

As the level of partial premixing decreases the fuel stream dilution becomes progressively less effective, while the air stream dilution becomes more effective in extinguishing the flame. Therefore, for flames exhibiting a double flame structure (i.e., $f_s > 0.5$) fuel stream dilution is more effective than air stream dilution, because the deficient reactant is the fuel. Conversely, for flames exhibiting a single flame structure (i.e., $f_s < 0.5$) air stream dilution is more effective since the deficient reactant is oxygen.

In microgravity the flame liftoff height and the critical CO_2 mole fraction at flame blow out are reduced due to the decrease in the effective gas stream velocity and the stretch rate at the flamefront.

For fuel stream diluted PPFs and air stream diluted NPFs, both thermal and dilution effects are present. Consequently, these flames are more easily extinguished compared to the corresponding air stream diluted PPFs and fuel stream diluted NPFs, since only thermal effects are dominant when extinguishing these latter flames.

Despite the different configurations, there is remarkable similarity in the extinction characteristics of coflow and

counterflow flames with regards to the effects of partial premixing and air stream and fuel stream dilutions.

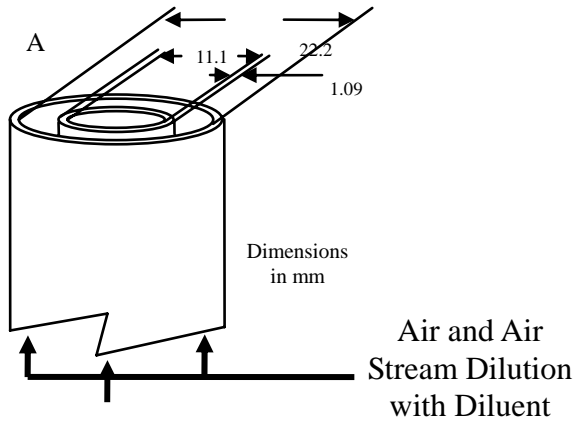
Ethylene-air flames are shown to have much the same dilution and extinction behavior as that observed for methane-air flames. Ethylene-air flame extinction diluent mole fractions are consistently higher than those for methane-air flames. The transition from fuel stream dominate dilution to air stream dominate dilution occurs at a larger equivalence ratio for ethylene-air flames than it does for methane-air flames. Air stream dilution may not suppressing ethylene air flames at an equivalence ratio below where fuel stream and air stream critical mole fractions are the same.

ACKNOWLEDGMENTS

This research was supported by the NASA Microgravity Research Division through Grant No. NCC3-688 for which Dr. Kurt Sacksteder serves as the technical monitor. Andrew Lock was supported by a fellowship through the NASA Graduate Student Research Program.

REFERENCES

- [1] Peters, N., Proc. Combust. Inst. 20 (1984) 353-360.
- [2] Seshadri, K., Puri, I. K., and Peters, N., Combust. Flame 61 (1985) 237-249.
- [3] Tsuji, H., Prog. Energ. Combust. Sci. 8 (1982) 93-119.
- [4] Hamins, A., Trees, D., Seshadri, K., Chelliah, H., Combust. Flame 99 (1994) 221.
- [5] Bundy, M., Hamins, A., Lee, K. Y., Combust. Flame 133 (2003) 299-310.
- [6] Trees, D., Grudno, A., Seshadri, K., Combust. Sci. Technol. 124 (1997) 311-330.
- [7] Vahdat, N., Zou, Y., Collins, M., Fire Safety J. 38 (2003) 553-567.
- [8] UNEP, Montreal Protocol on Substances that Deplete the Ozone Layer, 2004.
- [9] Law, C. K., Faeth, G. M., Prog. Energy Combust. Sci. 20 (1994) 65-113.
- [10] Lock, A. J., Ganguly, R., Puri, I. K., Aggarwal, S. K., Hedge, U., Proc. Combust. Inst. 30 (2004) 511-518.
- [11] Seiser, R., Truett, L., Seshadri, K., Proc. Combust. Inst. 29 (2002) 1551-1557.
- [12] Masri, A.R., Combust. Sci. Tech, Vol. 96, 1994, pp. 189-212
- [13] Trees, D., Grudno, A., Seshadri, K., , Combust. Sci. Tech. Vol. 124, 1997, pp. 311-330
- [14] Lock, A., Briones, A.M., Qin X, Aggarwal S.K., Puri I.K., Hegde U, *Combust Flame* 143 (2005) 159-173
- [15] Cho, Y. T., Na, S-J., Meas. Sci. Technol. 16 (2005) 878-884
- [16] Shu, Z., Aggarwal, S. K., Katta, V. R., Puri, I. K., Combust. Flame 111 (1997) 276.
- [17] Azzoni, R., Ratti, S., Puri, I. K., Aggarwal, S. K., Phys. Fluids 11 (1999) 3449.
- [18] Siegel, R., Howell, J. R., Thermal Radiation Heat Transfer, Hemisphere Publishing Corporation, New York, 1981.
- [19] Peters, N., Reduced Kinetic Mechanisms for Applications in Combustion Systems, Lecture Notes in Physics, Vol. m15, edited by N. Peters and B. Rogg, (Springer, Berlin, 1993), pp. 3-14.
- [20] Katta, V.R., Takahashi, F., Linteris, G.T., Combust. Flame 137 (2004) 506.
- [21] Kee, R. J., et. al, CHEMKIN Release 4.0.2, Reaction Design, San Diego, CA (2005).
- [22] Frenklach, M., Bowman, C.T., Smith, G.P., Gardiner, W.C., World Wide Web location http://www.me.berkeley.edu/gri_mech/, Version 3.0, 1999.
- [23] Li, S. C., Williams, F. A., "NOx formation in two-stage methane-air flames", Combust. Flame, 118:399-411 (1999)
- [24] Katta, V.R., Meyer, T.R., Brown, M.S., Gord, J.R., Roquemore, W.M., Combust. Flame 137 (2004) 198.
- [25] Shu, Z., Krass, B., Choi, C., Aggarwal, S. K., Katta, V., Puri, I. K., Proc. Combust. Inst. 27 (1998) 625.
- [26] Bilger, R. W., Proc. Combust. Inst. 22 (1988) 475.
- [27] Du, J., Axelbaum, R. L, Proc. Combust. Inst. 26 1137-1142 (1996)
- [28] Peters, N., Williams, F. A., AIAA J. 21 (1983) 423.



Rich Fuel/Air Mixture and Fuel Stream Dilution with Diluent

B



Fig. 1: Schematic diagram of the coflow burner (top: Fig. 1A). Image of the microgravity drop rig (bottom: Fig. 1B).

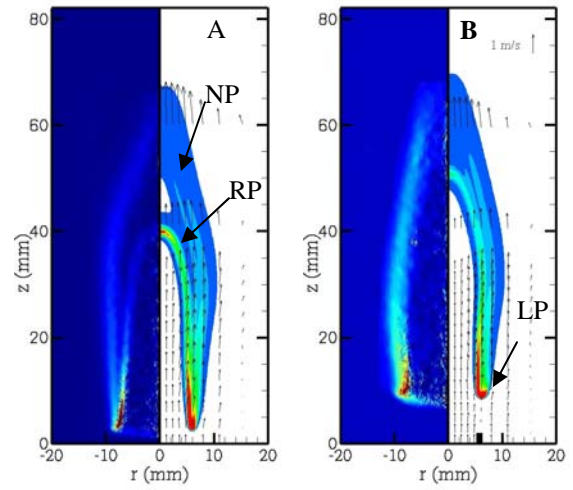


Fig. 2: Comparison of measured C_2^* chemiluminescence images (left) and predicted heat release rate contours (right) for undiluted (Flame A) and fuel stream CO_2 -diluted (Flame B, $X_{CO_2}=0.10$), lifted PPFs established at $\phi=2.25$. Velocity vectors are also shown for the simulated flames.

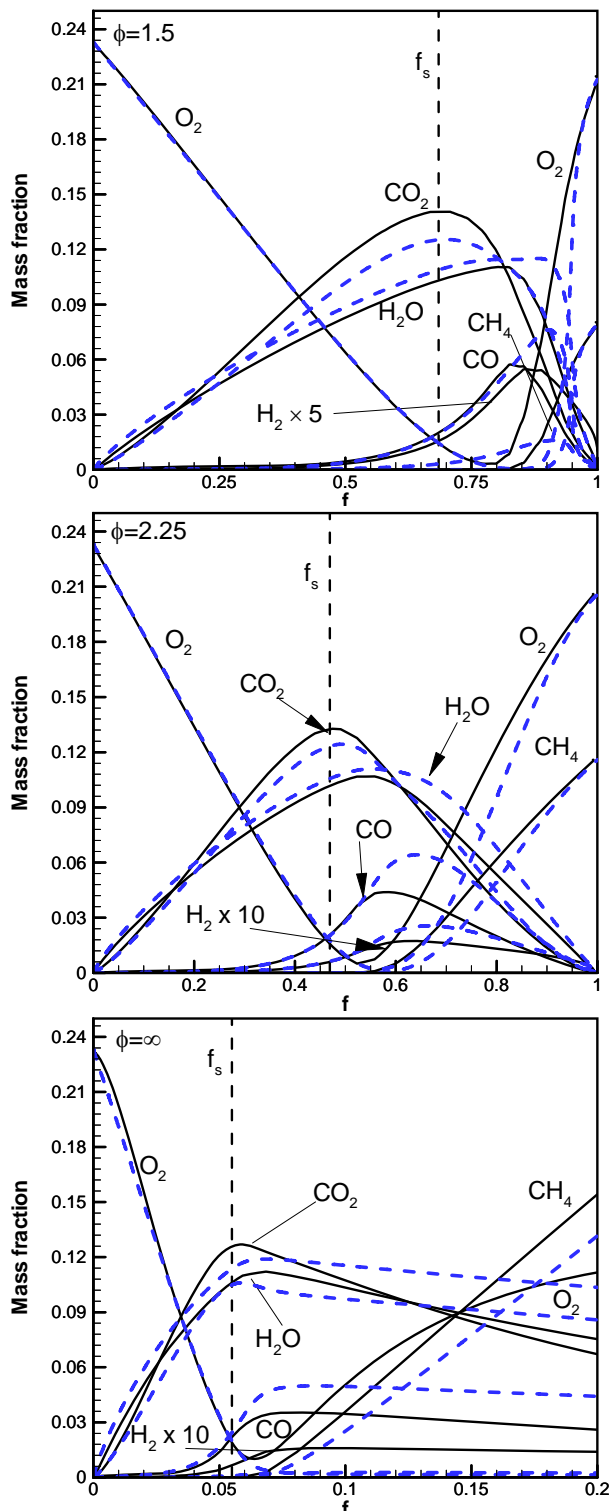


Fig. 3: State relationships in terms of scalar profiles at 2mm above the flame base, versus mixture fraction (f) for the coflow PPFs (at $\phi=1.5$, and 2.25) and NPF ($\phi=\infty$) (Blue Dashed Lines). Analogous steady counterflow partially premixed flames at a global strain rate of 100 s^{-1} are compared (Black Solid Lines).

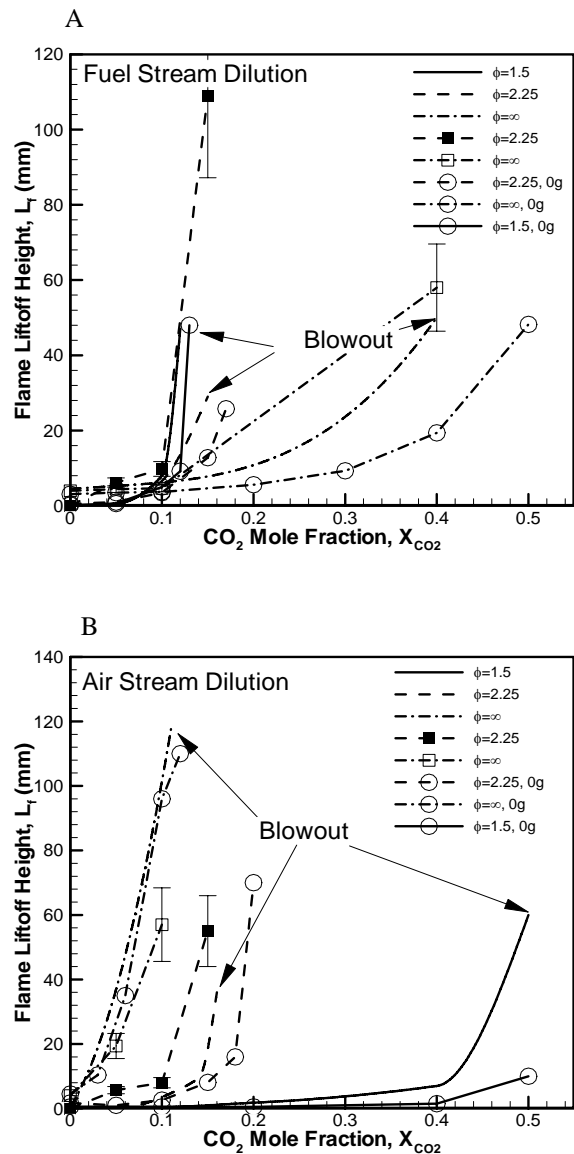


Fig. 4: Predicted 1-g (lines) and measured 1-g (lines with open and closed squares) and 0-g (lines with open circles) liftoff height (L_f) plotted as a function of CO_2 mole fraction for the fuel (top: Fig. 4A) and air (bottom: Fig. 4B) stream diluted, coflow PPFs (at $\phi=1.5$, and 2.25) and NPF. The 1-g blowout conditions are also shown.

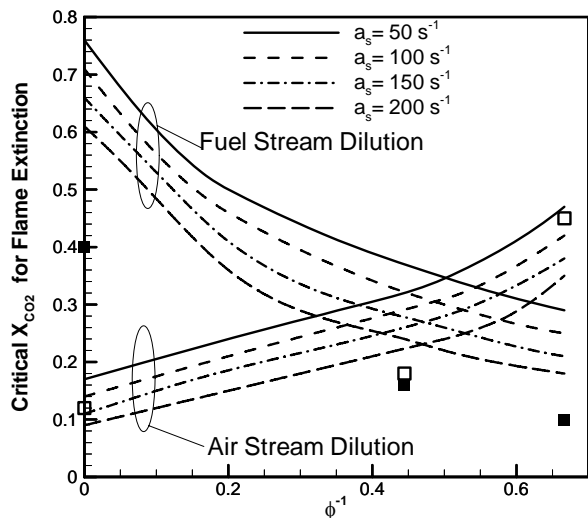


Fig. 5: Critical CO₂ mole fraction for the extinction of fuel and air stream diluted coflow and counterflow methane-air flames, plotted as a function of ϕ^{-1} . □ = air stream diluted coflow flames, ■ = fuel stream diluted coflow flames.

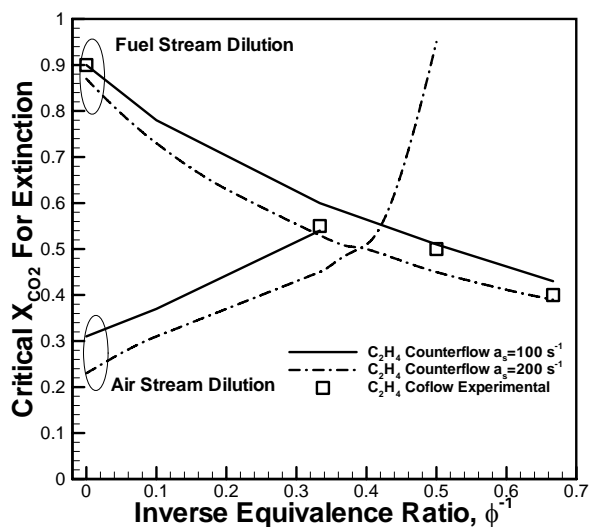


Fig. 6: Critical CO₂ mole fraction, required for the extinction of fuel and air stream diluted coflow and counterflow ethylene-air flames, plotted as a function of ϕ^{-1} , global strain rates $a_s=100 \text{ s}^{-1}$ and $a_s=200 \text{ s}^{-1}$.

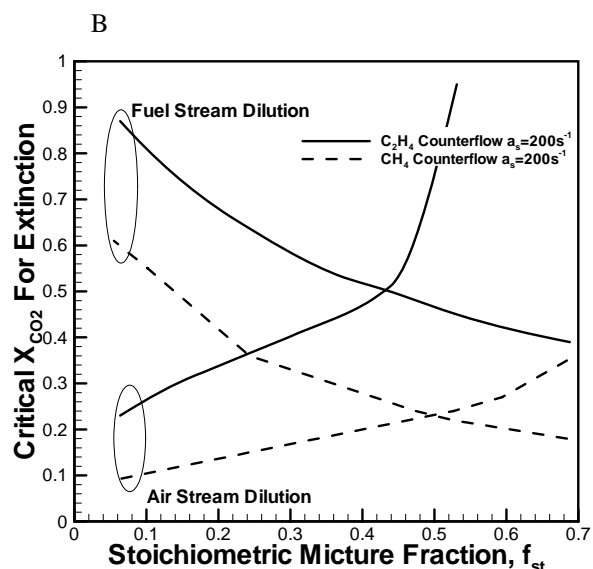
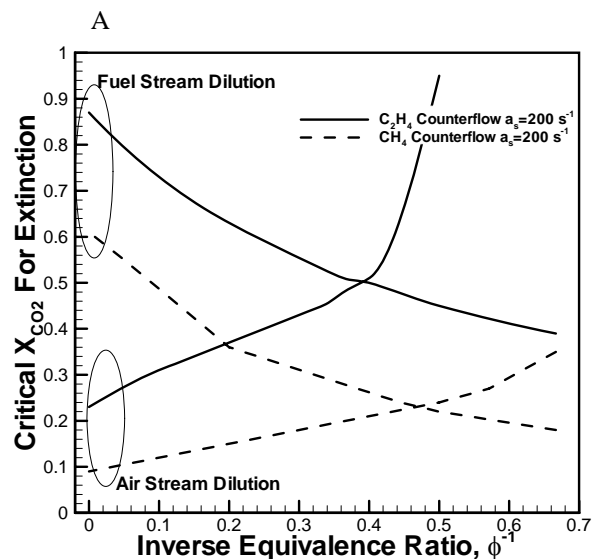


Fig. 7: Comparison of the extinction mole fraction, X_{CO_2} , for methane, CH₄, and Ethylene, C₂H₄, plotted versus inverse equivalence ratio, ϕ^{-1} , (top: Fig. 7A), and Stoichiometric Mixture Fraction, f_{st} , (bottom: Fig. 7B).